Modulation and Refinement of In–N re-Bonding of InGaN Through in Post-Flow During a Refined Temper Fire Treatment Process

TSUNG-YEN LIU [1], **LUNG-CHIEN CHEN** [2], **(Member, IEEE), CHENG-CHE LEE** [3], **YU CHENG** [4], **CHIEH-HSIUNG KUAN** [1,3], **(Member, IEEE), AND RAY-MING LIN** [4,5]

[1] Graduate Institute of Photonics and Optoelectronics, National Taiwan University, Taipei 10617, Taiwan, R.O.C.
[2] Graduate Institute of Electro-Optical Engineering, National Taipei University of Technology, Taipei 10608, Taiwan, R.O.C.
[3] Graduate Institute of Electronics Engineering, National Taiwan University, Taipei 10617, Taiwan, R.O.C.
[4] Department of Electronic Engineering and Institute of Electronics Engineering, Chang Gung University, Taoyuan 33302, Taiwan, R.O.C.
[5] Department of Radiation Oncology, Chang Gung Memorial Hospital, Linkou 33305, Taiwan, R.O.C.

Corresponding authors: Chieh-Hsiung Kuan (chkuan@ntu.edu.tw) and Ray-Ming Lin (rmlin@mail.cgu.edu.tw)

ABSTRACT In this article, we describe a subtle method for modulating and refining the indium–nitrogen (In–N) re-bonding effect of InGaN by employing an In post-flow during temper fire ($\Delta T = 110\,°C$) treatment. After optimizing the In flow rate and the temper fire treatment process, the In content in InGaN quantum wells (QWs) increased from 12.7 to 22.3% and the (102) epitaxy quality of InGaN improved, as revealed by the full-width at half-maximum (FWHM) of the X-ray diffractometry signal decreasing from 410 to 374 arcsec. In addition, the quality of a five InGaN/GaN multiple-QW epilayer surface also improved greatly when applying this technique. Merely by modulating the In post-flow rate (0, 5.6, 11.2, 16.8, 22.4, or 28.0 μmol/min), the In$_x$Ga$_{1-x}$N photoluminescence signal (and FWHM) changed from 449 nm (58 nm) in the absence of In post-flow during the temper fire treatment process, to 523 nm (46 nm) when the In post-flow rate was 11.2 μmol/min, and to 534 nm (55 nm) when the In post-flow rate was 28.0 μmol/min. This technique is, therefore, effective at improving the InGaN quality and compensating for the In–N bond desorption rate.

INDEX TERMS GaN, InGaN-based green LEDs, Indium–nitrogen re-bonding, refinement, metal–organic vapor phase epitaxy.

I. INTRODUCTION

Light emitting diodes (LEDs) have become pervasive in our daily lives since the invention of the InGaN-based blue LED (which achieves white light in conjunction with a yellow phosphor) completed the set of LEDs of the three primary colors (RGB). Nevertheless, the materials selected for the various emission wavelengths in RGB LEDs have several limitations. For example, in green LEDs, conventional iso-electronic doping with GaP:N leads—because of the indirect band gap—to a low external quantum efficiency (EQE). Upon increasing the content of aluminum in AlGaInP, the direct energy band gap is increased and the emission wavelength becomes shorter, resulting in the light emission efficiency becoming higher than that of GaP-based LEDs. Nevertheless,

The associate editor coordinating the review of this manuscript and approving it for publication was Jiajie Fan.

when with the aluminum content is too high (near to the green band), the weak conduction band discontinuity results in a dramatic decrease in the EQE. InGaN has been used successfully in blue-band LEDs, but increasing the In content, aiming for a longer emission wavelength, can cause the EQE to decrease, due to the lower quality of the InGaN quantum wells (QWs) and a phase separation effect in the InGaN. [1] Although nitride-based materials have provided emission wavelengths of up to 740 nm, there remain a need to improve the performance. [2] Furthermore, for micro-LEDs, the self-emission of a AlGaInP red LED has yet to be realized. If we could overcome this obstacle, InGaN would appear to be the best candidate material for RGB self-emission LEDs, allowing the realization of all nitride-based micro-LED displays. [3]

Many breakthroughs have been made in extending the emission of InGaN to longer wavelengths (toward the green

wavelength). For example, increasing the thickness and quality of the GaN buffer layer appears to be suitable for improving the performance of next-generation devices. [4]–[6] Hangleiter *et al.* generated V-pits in an InGaN/GaN superlattice (SL) structure to release the strain in the InGaN active region; these V-pits, which originated from threading dislocations, also enhanced carrier injection, screening dislocations, and radiative recombination. [4], [7]–[9] Common approaches for improving the crystalline quality of InGaN active layers include the use of two-step high-temperature growth and hybrid structures. Saito *et al.* reported that two-step high-temperature growth, with different growth temperatures for the well and the barrier layer, improved the flatness of the barrier layer and maintained the uniformity of the thickness of the QW layer in the case of multi-layer growth. [10]–[13] When the growth temperature of the barrier was higher than that of the well, the quality of the barrier improved to led to superior InGaN QWs; this approach was especially useful for preparing multiple quantum well (MQW) LEDs. Unfortunately, the In bonds undergo greater desorption during the temperature ramping process. To depress the rate of In desorption, Hubáčeka *et al.* developed some subtle methods for varying both the GaN and InGaN cap layer thicknesses at the InGaN QW growth temperature. [12] The optimal conditions—employing a thinner InGaN composition cap layer and no interruption during the temperature ramping process—resulted in the signal in the photoluminescence (PL) spectrum changing from 410 to 450 nm. Thus, the presence of an InGaN QW capping layer can suppress the desorption of In during the temperature ramping process. Nevertheless, the quality of the capping layer remains poor when using a low growth temperature, potentially seriously affecting the quality of the next InGaN QW.

The challenge remains to maintain the InGaN/GaN QW under compressive strain and improve the InGaN crystal quality which ensuring a high In content in the InGaN QW. The concept of a repaired weak bonding method (balancing the desorption rate and re-bonding rate) for chemical equilibrium has been developed. In this article, we demonstrate a subtle method for modulating and refining the In–nitrogen (In–N) re-bonding effect of InGaN by employing an In post-flow during the temper fire treatment process ($\Delta T = 110\,°C$). Under our optimal experiment conditions, we obtained high quality InGaN with a high In content in an efficient manner. Moreover, this method effectively compensated for the rate of InN desorption.

II. EXPERIMENTAL

All the samples were grown on *c*-plane sapphire substrates in a triple-layer horizontal-flow Nippon Sanso SR-2000 metal–organic vapor phase epitaxy (MOVPE) system under atmospheric pressure. For growth of the GaN buffer layer, hydrogen (H_2) was used as the carrier gas and trimethylgallium (TMGa) and ammonia (NH_3) were used as the Ga and N precursors, respectively. For growth of the


FIGURE 1. The full structure of samples.

MQWs, nitrogen (N_2) was used as the carrier gas and triethylgallium (TEGa) and trimethylindium (TMIn) were used as the Ga and In precursors, respectively. Fig. 1 presents the structure of the samples. A four-μm-thick GaN layer was prepared in two steps; first, a low-temperature nucleation layer was deposited and then a high-temperature buffer layer was formed on the sapphire substrate. [14]–[17] The following blue band QW layers featured two pairs of GaN layers and a lower-In-content $In_{0.12}Ga_{0.88}N$ QW for strain modulation and reduce the effect of piezoelectric field on the subsequent InGaN MQW layer. Iida *et al.* reported that a high-In-content InGaN active layer exhibits two peak emissions, attributed to phase separation in the InGaN layers; an InGaN medium QW layer hybrid structure can not only suppress these emissions almost completely but also result in narrower full-widths at half-maximum (FWHMs) in the spectra of the InGaN active QW. [11] Finally, the active region was formed from five pairs of two-step MQWs on the strain modulation blue band, each consisting of an $In_{0.22}Ga_{0.78}N$ well layer (3 nm) and a GaN barrier layer (10 nm). The growth temperature of each GaN barrier was 110 °C higher than that of the InGaN QWs, with the temper ramp time maintained at 3 min. For the structures described above, the TEGa and TMIn source flows were identical, but different TMIn supply post-flows were tested during the temperature ramping time (180 s) during the growth of the GaN barrier. Fig. 2 provides the temperature and TMIn flow profiles for the formation of the active layer. Fig. 2(a) displays the control sample A (in Table 1) flow profile; the growth temperatures for the InGaN QW and GaN barrier were 720 and 830 °C, respectively. After growth of the QW layer, the temperature was ramped to 830 °C without a TMIn source post-flow. Fig. 2(b) presents the profiles of the other treatment group samples; various TMI source post-flow rates (5.6, 11.2, 16.8, 22.4, 28.0 μmol/min) were applied during the course of temperature ramping, with all other growth conditions remaining identical.

The crystal quality of the GaN in each sample was determined from symmetric (002) and asymmetric (102)

TABLE 1. TMI Post-Flow Rates During the Temperature Ramping Period and Corresponding XRD Measurement Data and Dislocation Densities.

Sample	TMI flow (μmol/min)	(002) FWHM (arcsec)	(102) FWHM (arcsec)	D_{screw} ($10^7 cm^{-2}$)	D_{edge} ($10^8 cm^{-2}$)
A (control)	0	208.8	410.0	4.24	4.32
B	5.6	205.2	385.2	4.09	3.81
C	11.2	208.8	388.8	4.24	3.88
D	16.8	216.0	385.2	4.53	3.81
E	22.4	208.8	381.6	4.24	3.74
F	28.0	219.6	374.4	4.68	3.60

(a) (b)
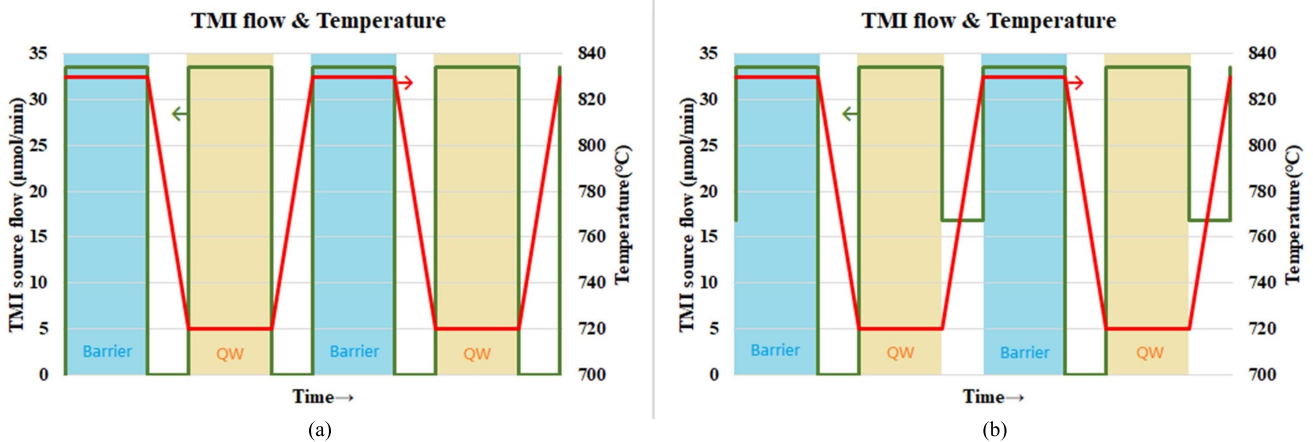
FIGURE 2. Temperature and TMIn source post-flow profiles of (a) the control sample (without a TMIn source post-flow during the temperature ramping period) and (b) the treatment samples (with various TMIn source post-flow rates during the temperature ramping period).

ω-scans measured using high-resolution X-ray diffractometry (HR-XRD, PANalytical X'Pert). PL spectroscopy was used to define the QW emission wavelength and optical quality and to determine the InGaN band gap (E_g) by neglecting the InGaN potential reaction with Vegard's law. A semiconductor pulsed laser emitting at 248 nm was used for PL excitation. Finally, the epitaxy of the surface morphology and the relative In content were determined using atomic force microscopy (AFM) and secondary ion mass spectrometry (SIMS), respectively.

III. RESULTS AND DISCUSSION

Table 1 presents the XRD measurement data and calculated dislocation densities of all of the samples prepared with different TMI post-flow flow rates during the temperature ramping process. Fig. 3 reveals the effect of the TMIn flow on the PL peak wavelength for each sample. Within the active layer, the electron–hole radiation rate will be affected directly by the QW crystalline quality and the confined potential barrier. A two-step high-temperature growth process is used commonly to improve the LED efficiency; a higher growth temperature for the barrier can not only significantly ameliorate the flatness of the GaN barrier surface and the crystalline quality but also meet the minimum quality requirements for subsequently formed InGaN QWs. In Table 1, sample A represents the control sample. During the growth
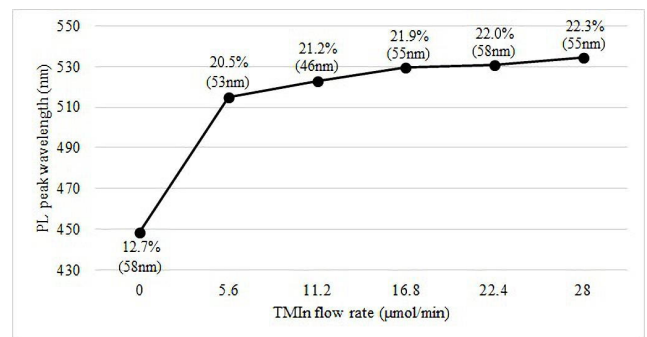
FIGURE 3. PL peak wavelength and In content for each sample; the PL spectral FWHM is presented under each In content.

of the five QWs, the InGaN wells were prepared at 720 °C and then the temperature for GaN barrier growth was ramped up to 830 °C. During the interruption period, the flows of both TEGa and TMIn were closed while waiting for the growth temperature to reach 830 °C as the conditions for the growth of the next barrier. Notably, the device target emission wavelength was set within the green band, but the PL peak wavelength in Fig. 3 reveals that the emission wavelength of sample A was approximately 449 nm—that is, it had shifted to the blue band.

The In content in the InGaN QW had decreased dramatically in sample A relative to other samples, presumably

because of desorption of the In–N bonds during the period of temperature ramping, where the InNbonding electrons possessed sufficient energy to escape, such that a desorption mechanism occurred and the In content of InGaN decreased rapidly. Although some previous reports have indicated that the use of an InGaN low-temperature QW cap layer can suppress the rate of In desorption [12], the alloy arrangement and crystal quality of the binary GaN material were superior to those of the ternary InGaN materials. To improve the quality of InGaN MQWs, we sought to decrease the rate of In–N bond desorption and to establish an In–N re-bonding process closer to thermal equilibrium by refining the temper fire treatment process. While maintaining the temperature ramp time between the QW and the barrier at 3 min, we wished to compensate for more desorption of In–N weak bonds during the temperature ramping time with more stable In–N re-bonding. Thus, all of the other samples retained the same structure as sample A, but we employed different TMIn source post-flow rates during the period of temperature ramping as a subtle method for refining the temper fire treatment of In–N bonds. Table 1 provides the TMIn source post-flow rates and XRD measurement data of all of our samples. We obtained samples B–F with post-flow rates set at 5.6, 11.2, 16.8, 22.4, and 28.0 μmol/min, respectively. We used the FWHMs of the symmetric (002) and asymmetric (102) signals to estimate the screw and edge densities of dislocation, using the relationships [18]–[20]

$$D_{screw} = \frac{FWHM^2_{(002)}}{9b^2_{screw}} \qquad (1)$$

$$D_{edge} = \frac{FWHM^2_{(102)}}{9b^2_{edge}} \qquad (2)$$

where D is the dislocation density and b is the Burgers vector. The calculated dislocation densities (Table 1) reveal that the densities of the screw dislocations for all of our samples were similar. We suspect that the In desorption process was mostly related to the formation of edge dislocations, whose Burgers vectors were aligned along the QW–barrier interface, leaving the symmetric (002) planar spacing essentially undistorted. Because the density of edge dislocations was mostly reflected by the FWHM of the asymmetric (102) value, the effect of introducing the TMIn post-flow into the reactor chamber was manifested by the decreasing values of D_{edge} in Table 1. For samples B–F, the contents of edge-type dislocations were 11–16% lower than that in sample A, which was prepared without the TMIn post-flow introduced into the reactor chamber. Fig. 3 also presents the relationship between the TMIn post-flow rate during temperature ramping and the PL spectral peak wavelength. The PL spectral peak wavelength shifted to substantially longer wavelength—from the blue-violet (449 nm) to the blue-green (534 nm)—when the TMIn post-flow was introduced during the period of interruption. The lateral growth mode is most determined by growth temperature. But how to control the InGaN desorption rate is very critical in InGaN. We have executed both to

depress the InGaN MQW desorption rate and also increase the indium atom migration length.

In the absence of the TMIn post-flow during the interruption period, the PL spectral peak wavelength appeared at 449 nm and the corresponding In content was 12.7%. We calculated the InGaN In content by using the Schrödinger wave equation with a quantized level shift (will be published later) and following Vegard's law, estimated as follows:

$$E_{g,InGaN}(x) = xE_{g,InN} + (1-x)E_{g,GaN} - bx(1-x) \qquad (3)$$

where $E_{g,InGaN}(x)$, $E_{g,InN}$, and $E_{g,GaN}$ represents the band gaps of InGaN, InN, and GaN, respectively, at room temperature and b (equal to 2.8 eV) is the bowing parameter for InGaN. [21], [22] When the TMIn post-flow rate during the temperature ramping period was 5.6 μmol/min, the PL spectral peak wavelength increased to 515 nm and the FWHM decreased from 58 nm (sample A) to 52 nm (sample B). In general, the FWHM of the PL spectral signal was inversely related to the PL spectral emission band gap. Sample A had an In content lower than that of sample B, but the FWHM of the PL spectral signal of sample B was less than that of sample A. Thus, through modulation and refinement of the In–N re-bonding of the InGaN by applying an In post-flow during the temper fire treatment process, we could greatly increase both the In content of the InGaN and, astonishingly, the epitaxial quality of the InGaN QW. When we increased the TMIn post-flow further, the PL spectral signal underwent a continuous shift to a longer wavelength, due to a greater In–N re-bonding effect during the ramping period. Nevertheless, the peak wavelength shift became increasingly saturated upon proceeding from sample B to sample F, indicating that not only the rate of In–N bond desorption suppressed effectively but also more compensating In–N bonds were formed. The optimal sample was that formed when the post-flow rate was 11.2 μmol/min, with the PL spectral emission peak and the FWHM being 523 and 46 nm, respectively. When the flow rate was saturated at 16.8 μmol/min, the PL spectral emission peak appeared at 530 nm, corresponding to an In content of 21.9%. The PL spectral data suggested that the introduction of the TMIn post-flow into the chamber suppressed the In desorption significantly, by at least 8%. We want to breakthrough the destiny of the InGaN growth with high indium composition temperature limited. As we know, the bounding site will turn better with the growth of increased temperature. So, in our study, we refined the indium-nitrogen (In–N) re-bonding effect of InGaN by employing an In post-flow during temper fire ($\Delta T = 110 \,^{\circ}C$) treatment. From PL data, we have to make sure the weak bonding of InGaN immediately desorption during the temper fire process and re-bonding a better bonding site of InGaN with the In-post flow rate method, which could effectively compensate for the weak bonding InGaN desorption rate and also increase the InGaN bonding energy. We used AFM to evaluate the surface morphologies of our samples. Fig. 4(a) reveals an average surface roughness (Ra) of 1.48 nm for the sample prepared without introducing a TMIn post-flow into
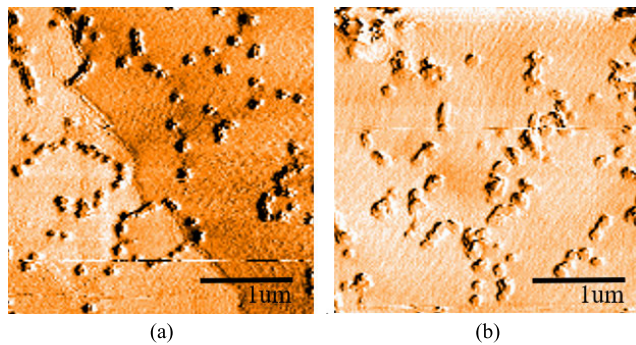
FIGURE 4. AFM images of samples prepared (a) without a TMIn post-flow and (b) with a TMIn post-flow (22.4 μmol/min) introduced during the temperature ramping process.

the chamber during temperature ramping period; when the TMIn post-flow was introduced into the chamber at a rate of 22.4 μmol/min during the period of temperature ramping, the value of Ra decreased significantly, to 1.09 nm [Fig. 4(b)]. This behavior is consistent with the XRD data, which suggested that the introduced TMIn post-flow not only decreased the dislocation density but also led to a smoother surface morphology. Finally, we used SIMS to measure the relative In contents. The SIMS data (not shown here) revealed that the In/Ga concentration ratio in the InGaN QWs increased upon increasing the depth. Thus, by applying an TMIn post-flow during a refined temper fire treatment process, we could not only compensate for the rate of In–N bond desorption but also enrich the sample with In–N bonds. In the QW region, the In content of the sample prepared with an introduced TMIn post-flow was six times higher than that of the sample prepared without the TMIn post-flow.

IV. CONCLUSION

We have prepared InGaN MQW structures by applying an In post-flow during the period of interruption, thereby effectively compensating for the desorption of In–N bonds by enriching the In–N bonds and improving the epitaxial quality of the InGaN MQWs. After optimizing the In flow rate and refining the temper fire treatment process, the In content of the InGaN QWs increased from 12.7 to 22.3% and the (102) epitaxial quality improved, with of the FWHM of the XRD signal of the InGaN decreasing from 410 to 374 arcsec. Furthermore, the PL spectral FWHM was inversely related to the PL spectral emission band gap of the InGaN MQW. Although sample A had an In content lower than that of sample B, the PL spectral FWHM of sample B was less than that of sample A. Thus, through modulation and refinement of the In–N re-bonding process of InGaN samples by applying an In post-flow during a refined temper fire treatment process, we could greatly increase the In content in the InGaN samples astonishingly, and improve the epitaxial quality of the InGaN MQWs.

REFERENCES

[1] M. Rao, D. Kim, and S. Mahajan, "Compositional dependence of phase separation in InGaN layers," *Appl. Phys. Lett.*, vol. 85, no. 11, pp. 1961–1963, Sep. 2004.

[2] K. Ohkawa, T. Watanabe, M. Sakamoto, A. Hirako, and M. Deura, "740-nm emission from InGaN-based LEDs on c-plane sapphire substrates by MOVPE," *J. Cryst. Growth*, vol. 343, no. 1, pp. 13–16, Mar. 2012.

[3] J. J. Wierer and N. Tansu, "III-nitride micro-EDs for efficient emissive displays," *Laser Photon. Rev.*, vol. 13, no. 9, Sep. 2019, Art. no. 1900141.

[4] D. Iida, Z. Zhuang, P. Kirilenko, M. Velazquez-Rizo, M. A. Najmi, and K. Ohkawa, "633-nm InGaN-based red LEDs grown on thick underlying GaN layers with reduced in-plane residual stress," *Appl. Phys. Lett.*, vol. 116, no. 16, Apr. 2020, Art. no. 162101.

[5] S. Srinivasan, L. Geng, R. Liu, F. A. Ponce, Y. Narukawa, and S. Tanaka, "Slip systems and misfit dislocations in InGaN epilayers," *Appl. Phys. Lett.*, vol. 83, no. 25, pp. 5187–5189, Dec. 2003.

[6] M. Iwaya, T. Yamamoto, D. Iida, Y. Kondo, M. Sowa, H. Matsubara, K. Ishihara, T. Takeuchi, S. Kamiyama, and I. Akasaki, "Relationship between misfit-dislocation formation and initial threading-dislocation density in GaInN/GaN heterostructures," *Jpn. J. Appl. Phys.*, vol. 54, no. 11, Oct. 2015, Art. no. 115501.

[7] F. Jiang, J. Zhang, L. Xu, J. Ding, G. Wang, X. Wu, X. Wang, C. Mo, Z. Quan, X. Guo, C. Zheng, S. Pan, and J. Liu, "Efficient InGaN-based yellow-light-emitting diodes," *Photon. Res.*, vol. 7, no. 2, pp. 144–148, Feb. 2019.

[8] Q. Lv, J. Liu, C. Mo, J. Zhang, X. Wu, Q. Wu, and F. Jiang, "Realization of highly efficient InGaN green LEDs with sandwich-like multiple quantum well structure: Role of enhanced interwell carrier transport," *ACS Photon.*, vol. 6, no. 1, pp. 130–138, Dec. 2018.

[9] A. Hangleiter, F. Hitzel, C. Netzel, D. Fuhrmann, U. Rossow, G. Ade, and P. Hinze, "Suppression of nonradiative recombination by V-shaped pits in GaInN/GaN quantum wells produces a large increase in the light emission efficiency," *Phys. Rev. Lett.*, vol. 95, no. 12, Sep. 2005, Art. no. 127402.

[10] S. Saito, R. Hashimoto, J. Hwang, and S. Nunoue, "The Japan society of applied physics, find out more InGaN light-emitting diodes on C-face sapphire substrates in green gap spectral range," *Appl. Phys. Exp.*, vol. 6, no. 11, Oct. 2013, Art. no. 111004.

[11] D. Iida, K. Niwa, S. Kamiyama, and K. Ohkawa, "Demonstration of InGaN-based orange LEDs with hybrid multiple-quantum-wells structure," *Appl. Phys. Exp.*, vol. 9, no. 11, Oct. 2016, Art. no. 111003.

[12] T. Hubáček, A. Hospodková, J. Oswald, K. Kuldová, J. Pangrác, M. Zíková, F. Hájek, F. Dominec, N. Florini, P. Komninou, G. Ledoux, and C. Dujardin, "Strong suppression of in desorption from InGaN QW by improved technology of upper InGaN/GaN QW interface," *J. Cryst. Growth*, vol. 507, pp. 310–315, Feb. 2019.

[13] D. Iida, S. Lu, S. Hirahara, K. Niwa, S. Kamiyama, and K. Ohkawa, "Enhanced light output power of InGaN-based amber LEDs by strain-compensating AlN/AlGaN barriers," *J. Cryst. Growth*, vol. 448, pp. 105–108, Aug. 2016.

[14] S. Nakamura, "GaN growth using GaN buffer layer," *Jpn. J. Appl. Phys.*, vol. 30, pp. 1705–1707, Oct. 1991.

[15] Z.-T. Li, K. Cao, J.-S. Li, Y. Tang, L. Xu, X.-R. Ding, and B.-H. Yu, "Investigation of light-extraction mechanisms of multiscale patterned arrays with rough morphology for GaN-based thin-film LEDs," *IEEE Access*, vol. 7, pp. 73890–73898, Jun. 2019.

[16] S. Nakamura, M. Senoh, N. Iwasa, and S. Nagahama, "High-brightness InGaN blue, green and yellow light-emitting diodes with quantum well structures," *Jpn. J. Appl. Phys.*, vol. 34, pp. 797–799, Jul. 1995.

[17] S. J. Chang, W. C. Lai, Y. K. Su, J. F. Chen, C. H. Liu, and U. H. Liaw, "InGaN-GaN multiquantum-well blue and green light-emitting diodes," *IEEE J. Sel. Topics Quantum Electron.*, vol. 8, no. 2, pp. 278–283, Aug. 2002.

[18] P. Gay, P. B. Hirsch, and A. Kelly, "The estimation of dislocation densities in metals from X-ray data," *Acta Metallurgica*, vol. 1, no. 3, pp. 315–319, May 1953.

[19] X. H. Zheng, H. Chen, Z. B. Yan, Y. J. Han, H. B. Yu, D. S. Li, Q. Huang, and J. M. Zhou, "Determination of twist angle of in-plane mosaic spread of GaN films by high-resolution X-ray diffraction," *J. Cryst. Growth*, vol. 255, nos. 1–2, pp. 63–67, Jul. 2003.

[20] E. Arslan, M. K. Ozturk, A. Teke, S. Ozcelik, and E. Ozbay, "Buffer optimization for crack-free GaN epitaxial layers grown on Si(1 1 1) substrate by MOCVD," *J. Phys. D, Appl. Phys.*, vol. 41, no. 15, Jul. 2008, Art. no. 155317.

[21] V. K. Singh, P. Taya, D. Jana, R. Tyagi, S. Raghavan, and T. K. Sharma, "On the determination of alloy composition using optical spectroscopy in MOVPE grown InGaN layers on Si(111)," *Superlattices Microstructures*, vol. 134, Oct. 2019, Art. no. 106234.

[22] M. Moret, B. Gil, S. Ruffenach, O. Briot, C. Giesen, M. Heuken, S. Rushworth, T. Leese, and M. Succi, "Optical, structural investigations and band-gap bowing parameter of GaInN alloys," *J. Cryst. Growth*, vol. 311, no. 10, pp. 2795–2797, May 2009.

YU CHENG was born in New Taipei, Taiwan, in 1998. He received the B.S. degree in electron engineering from Chang Gung University, Taoyuan, in 2020. He is currently pursuing the master's degree with the Electron Engineering Department, Chang Gung University. His research interests include III-V-based light-emitting diodes (LEDs) and photo detector, optoelectronic components, and thin film technology.

TSUNG-YEN LIU was born in Taoyuan, Taiwan, in 1989. He received the B.S. degree in electrical engineering from Chunghua University, Hsinchu, Taiwan, in 2011, and the M.S. degree in electrical engineering from Tamkang University, Taipei, Taiwan, in 2013. He is currently pursuing the Ph.D. degree in photonics and optoelectronics engineering from National Taiwan University.

His research interests include III/IV compound semiconductor metal-organic chemical vapor deposition, deep-ultraviolet LED, high indium content InGaN-based yellow-green LED, and high electron mobility transistor (HEMT).

CHIEH-HSIUNG KUAN (Member, IEEE) was born in Taipei, Taiwan, in 1962. He received the B.S. degree in electrical engineering from National Taiwan University, in 1985, and the M.S.A. and Ph.D. degrees in electrical engineering from Princeton University, in 1990 and 1994, respectively. During his Ph.D. work, he was major in the dark current and noise characteristics of the infrared hot-electron transistors and cooperated with the U.S. Army Laboratory, Fort Monmouth, NJ, USA. In 1994, he joined as an Associate Professor with the Department of Electrical Engineering, National Taiwan University, where he was promoted as a Full Professor in 2002. His current research interests include the infrared photodiode for room temperature operation, the quantum well infrared photodetector and laser, superlattice infrared photodetector and the associated multi-color detector, and the topics on how to measure and suppress the noise in the detectors. He has set up E-beam and high-resolution microscope systems to research further in advanced lithography technology. The infrared detector, composed of two superlattices separated by a wide barrier and proposed by Dr. Kuan in 2002, was cited as a newsbreak in the June issue of Laser Focus World.

Dr. Kuan is a member of the IEEE Society and the Phi-Tau-Phi Honored Scholar Society.

LUNG-CHIEN CHEN (Member, IEEE) received the B.S. degree in electrical engineering from the National Taiwan University of Science and Technology, Taipei, Taiwan, in 1991, and the Ph.D. degree in electrical engineering from National Tsing Hwa University, Hsinchu, Taiwan, in 1999. In 2002, he joined as a Faculty Member with the Institute of Electro-Optical Engineering, National Taipei University of Technology, Taipei. He has authored or coauthored more than 145 SCI technical articles in 60 international conferences, and 180 conference papers. He holds more than 21 patents in his fields of expertise. His current research interests include the MOCVD, LPE, and solution CVD epitaxial growth techniques, fabrication, and analysis of III–V compound semiconductor/oxide semiconductor devices, fabrication and characterization of nanomaterials, light-emitting diodes (LEDs), sensors, solar cells, perovskite quantum dots, and perovskite optoelectronic devices.

RAY-MING LIN received the Ph.D. degree in electrical engineering from National Taiwan University, Taiwan, Republic of China, in 1997. During his Ph.D. work, he majored in the MBE growth and device application of metamorphic InGaAs/GaAs and InAlAs/GaAs buffer layers, quantum dot light emitting diode, and room temperature infrared sensor.

He spent his whole life thinking about and dreaming about only one kind of research-Epitaxy. From 1997 to 1999, he joined as an Assistance Research Fellow the Planning & Evaluation Division, National Science Council. Since August 1999, he has been with the Department of Electronic Engineering, Chang Gung University, Taoyuan, Taiwan, Republic of China, where he is currently a Full Professor. Since August 2001, he has been the Director of the Right and Technology Transfer Center, Chang Gung University. He has published more than 84 technical articles in reviewed archival journals. His current research interests include MOCVD technology development for the growth of Nitride-based heterostructures, *in-situ* fabrication of low-dislocation density, high-efficiency optoelectronic, and high electron mobility transistor (HEMT) device structures.

CHENG-CHE LEE received the B.S. and M.S. degrees in electronics engineering from the China University of Science and Technology, Taipei, Taiwan, in 2008 and 2010, respectively. He is currently pursuing the Ph.D. degree with the Graduate Institute of Electronics Engineering, National Taiwan University. He is also a Research Staff with the E-bema Laboratory, NTU GIEE. His research interests include E-beam lithography technology, III-V semiconductor electronic and optoelectronic devices integrated optics, and organic electronic devices.

• • •